

© Springer Science+Business Media LLC 2017

Robert A. Meyers

Encyclopedia of Complexity and Systems Science

10.1007/978-3-642-27737-5_677-1

Graphs Related to Reversibility and Complexity in Cellular Automata

Juan C. Seck-Tuoh-Mora¹ and Genaro J. Martínez²

(1)Instituto de Ciencias Básicas e Ingeniería, Área Académica de Ingeniería, Universidad Autónoma del Estado de Hidalgo, Ciudad del Conocimiento, Carretera Pachuca- Tulancingo Km. 4.5, Col. Carboneras, Mineral de la Reforma, C. P. 42184 Hidalgo, Mexico

(2)Escuela Superior de Cómputo, Instituto Politécnico Nacional, México Unconventional Computing Center, University of the West of England, Bristol, UK

Juan C. Seck-Tuoh-Mora

Email: jseck@uaeh.edu.mx

Without Abstract

Glossary

Cellular automaton

is a discrete dynamical system composed by a finite array of cells connected locally, which update their states at the same time using the same local mapping that takes into account the closest neighbors.

Complex automaton

is a cellular automaton characterized by generating complex structures in its spatial-temporal evolution. For instance, the formation of self-localizations or gliders.

Cycle graph

is a directed graph in which vertices are finite configurations and edges represent the global mapping between configurations induced by the local evolution rule.

De Bruijn graph

is a directed graph in which vertices represent partial neighborhoods and edges represent complete neighborhoods obtained by valid overlaps between vertices. Edges are labeled according to the evolution of the neighborhood.

Glider

is a complex pattern with volume, mass, period, displacement, and direction. Sometimes these nontrivial patterns are referred as particles, waves, spaceships, or mobile self-localizations.

Graph

is a set of vertices in which some pairs of them are related by edges. In the case that edges have direction, we have a directed graph.

Pair graph

is a directed graph in which vertices are pairs of de Bruijn vertices and there is a directed edge from one pair to the other if both vertices in the initial pair are linked to both vertices in the final pair with the same label in the de Bruijn graph.

Reversible automaton

is a cellular automaton in which the global mapping induced by the local evolution rule may be inverted by another evolution rule, possibly with different neighborhood size.

Subset graph

is a directed graph obtained from the power set of vertices in the de Bruijn graph including the empty set. There is a directed edge from one subset to other if at least one of the vertices in the initial subset are linked with the same label to all the vertices in the final subset, and this subset is maximal. If there is no subset holding this property, the edge goes to the empty set.

Surjective automaton

is a cellular automaton in which every finite sequence of cell-states has at least one possible preimage, that is, there are not Garden-of-Eden sequences.

Definition of the Subject

Concepts from graph theory have been used in the local and global analysis and characterization of a cellular automaton (CA). In particular, De Bruijn graph, pair graph, subset graph, and cycle graph have been employed to represent the local cell-state transition rules and their induced global transformations. These graphs are useful to analyze, classify, and construct interesting dynamics in one-dimensional CAs. Reversibility and complexity have been a common field of study where graphic tools have been successfully applied.

Introduction

The term *graph* used in this entry refers to a set of vertices in which some pairs of them are related by edges. In particular, most of the graphs reviewed are directed graphs (or digraphs), where edges have orientations Bang-Jensen and Gutin ([2008](#)).

The graph structure is a natural way to represent the states in time of interacting entities (agents, biological cells, molecules, and so on), where direct interaction between components (or vertices) is represented by an edge Mortveit and Reidys ([2007](#)).

A first application of graphs in automata theory was introduced by C. E. Shannon and W. Weaver using state diagrams to represent finite state machines Shannon ([2001](#)).

Graphs and digraphs have been widely used to represent, analyze, and characterize different types of automata Hopcroft ([1979](#)), Sakarovitch ([2009](#)), Khoussainov and Nerode ([2012](#)).

As H.V. McIntosh explains in McIntosh ([2009](#)), in CA theory, a diagrammatic technique for representing one-dimensional CAs lies at the heart of shift register theory Golomb et al. ([1982](#)).

In particular, for the one-dimensional case, the overlap of neighborhoods in a CA can be adequately represented by de Bruijn graphs. A de Bruijn graph is a directed graph where vertices are sequences of symbols and edges represent the overlaps between them de Bruijn ([1946](#)). In CAs, vertices are partial neighborhoods and edges represent complete neighborhoods labeled by the corresponding mapping defined in the evolution rule.

Well-known results of de Bruijn graphs in CA studies were presented by Nasu ([1977](#)) referring the properties of injective and surjective evolutionary functions to de Bruijn and related graphs; Wolfram ([1984](#)) characterizing evolutionary properties; and Jen ([1987](#)) to calculate ancestors.

The Cartesian product of a de Bruijn graph is useful to compare paths in the same graph looking for shared or special vertices. That is the idea behind the pair graph, used by McIntosh ([1991](#)) and Sutner ([1991](#)) to prove reversibility in one-dimensional CAs.

In automata theory, the power set construction (or subset graph) is a classical procedure to obtain a deterministic version of a nondeterministic finite automaton Moore ([1956](#)), Rabin and Scott ([1959](#)). In CAs, this method can be applied to de Bruijn graphs to analyze features of the set of sequences (or language) recognized by the graph.

An excellent application of the subset graph is to search Garden-of-Eden sequences, which cannot be produced from any other sequence during the evolution of a given CA. Other uses are calculating, counting, and computing the frequency distribution of the multiplicity of counterimages, results that are relevant to characterize a reversible automaton McIntosh ([2009](#)).

The evolution of a CA can be represented as well by a graph where each vertex represents a global state and transitions between them are depicted by directed edges. First we can enumerate all the sequences of the desired length and follow up the evolution of each induced by the evolution rule of the automaton. For small length sequences, periodicities can be detected very quickly through the cycles of this graph, whose lengths will give the periods of that length. This graphic representation of the automaton dynamics generates basins of attraction. The number, length, and shape of branches and cycles in this graph (the cycle graph) characterize the patterns formed by the automaton.

Cycle graphs and their basins of attraction were firstly used to characterize and compare different classification schemes of CA dynamics in Wuensche and Lesser ([1992](#)).

This entry is focused to present the most relevant graphs used to represent and analyze one-dimensional CAs. In particular, the definition and most relevant works of de Bruijn, pairs, subset, and cycle graphs are described in the study of reversible and complex automaton. There are other types of graphs such as Cayley, Voronoi, and jump graphs which are also important but have not been taken in consideration in this entry.

The document is organized as follows. Section “ [Basics on Cellular Automata and Related Graphs](#)” gives the basic concepts of one-dimensional CAs and examples of the most important graphs for reversible and complex automata. Section “ [De Bruijn Graph](#)” presents the most relevant results using de Bruijn graphs for reversible and complex automata. Section “ [Pair and Subset Graphs](#)” describes interesting applications of pair and subset graphs for CAs. Section “ [Cycles and Basins of Attraction](#)” depicts the important use of cycle diagrams for characterizing and classifying reversible and complex automata. The final section provides some further directions in the utilization of graphs in CA theory. The illustrations of this entry have been generated using the NXL-CAU software developed by Harold V. McIntosh. This software is a set of specialized packages, one for each type of one-dimensional CA, depending on the number of states and neighborhood radius. The software is available in <http://delta.cs.cinvestav.mx/~mcintosh/oldweb/software.html>

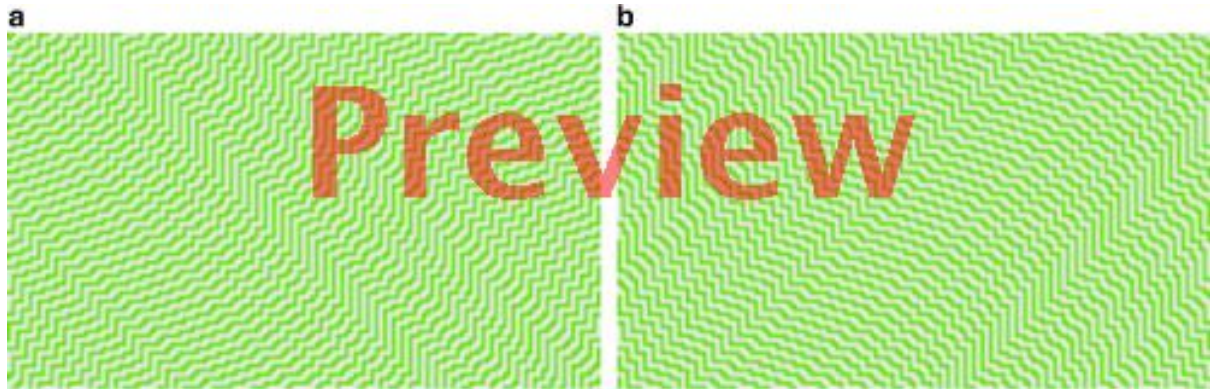
Basics on Cellular Automata and Related Graphs

A CA is composed by a finite set S of states, a neighborhood radius r , and an evolution rule $\varphi: S^{2r+1} \rightarrow S$. The dynamics of the automaton is initialized by an initial condition or configuration $\{(c)_i^0 = \{c\}_1^0 \{c\}_2^0 \dots \{c\}_n^0\}$ of n states, where $\{c\}_i^0 \in S$.

Every cell in $\{c\}_i^t$ has associated a neighborhood $\{\eta \left(\{c\}_i^t \right) = \{c\}_{i-r}^t \dots \{c\}_{i+r}^t\}$ in which periodic boundary conditions are commonly used. Thus, $\{c\}_i^{t+1} = \varphi \left(\eta \left(\{c\}_i^t \right) \right)$ and the evolution rule generates a global mapping $\Phi: S^n \rightarrow S^n$ between configurations.

A CA is reversible if given its evolution rule φ , there exists another rule φ^{-1} (possibly with a different neighborhood radius) such that the induced global mapping Φ^{-1} holds that $\Phi^{-1}(\Phi(c)) = c$. In other words, the dynamics of the automaton can be *reversed* by another evolution rule.

Elementary CA (ECA) rule 15 is a typical example of a reversible automaton, where rule 85 gives the inverse behavior (Fig. 1).



If you need to edit the image, please use the original: 126766_0_En_677-1_Fig1_Print.tif

Fig. 1

Example of spatial-temporal patterns of reversible ECA rule 15 (a) and rule 85 (b)

ECA rule 54 and rule 110 are classical examples of complex CAs characterized by spatial-temporal patterns conformed by self-localizations interacting in a periodic background (Fig. 2).

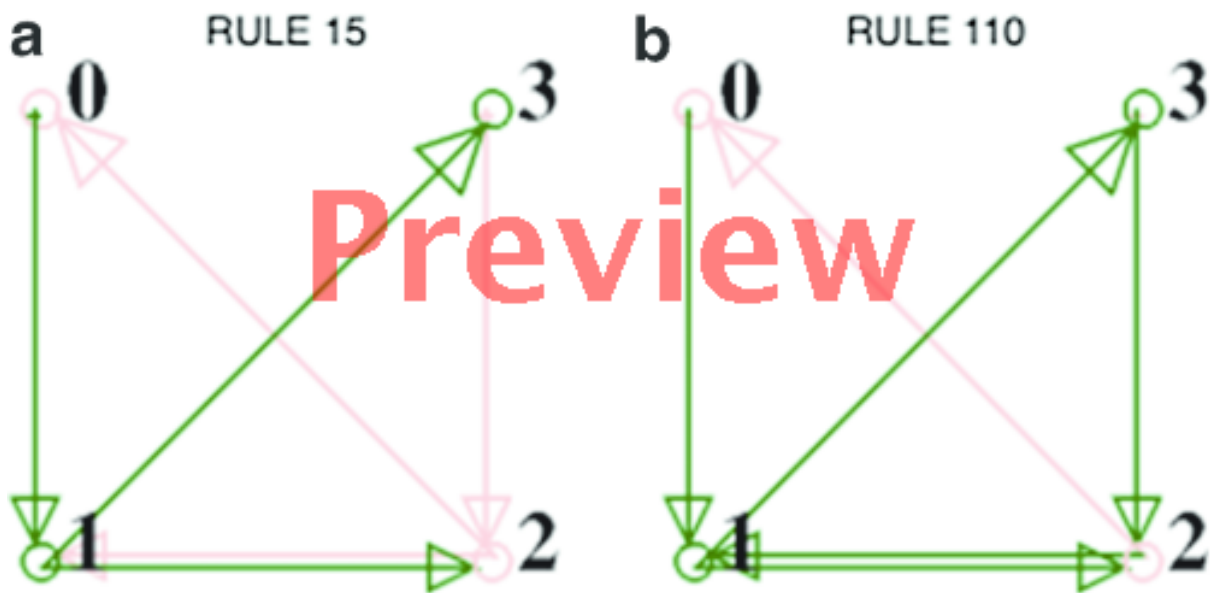


If you need to edit the image, please use the original: 126766_0_En_677-1_Fig2_Print.tif

Fig. 2

Example of spatial-temporal patterns of complex ECA rule 54 (a) and rule 110 (b)

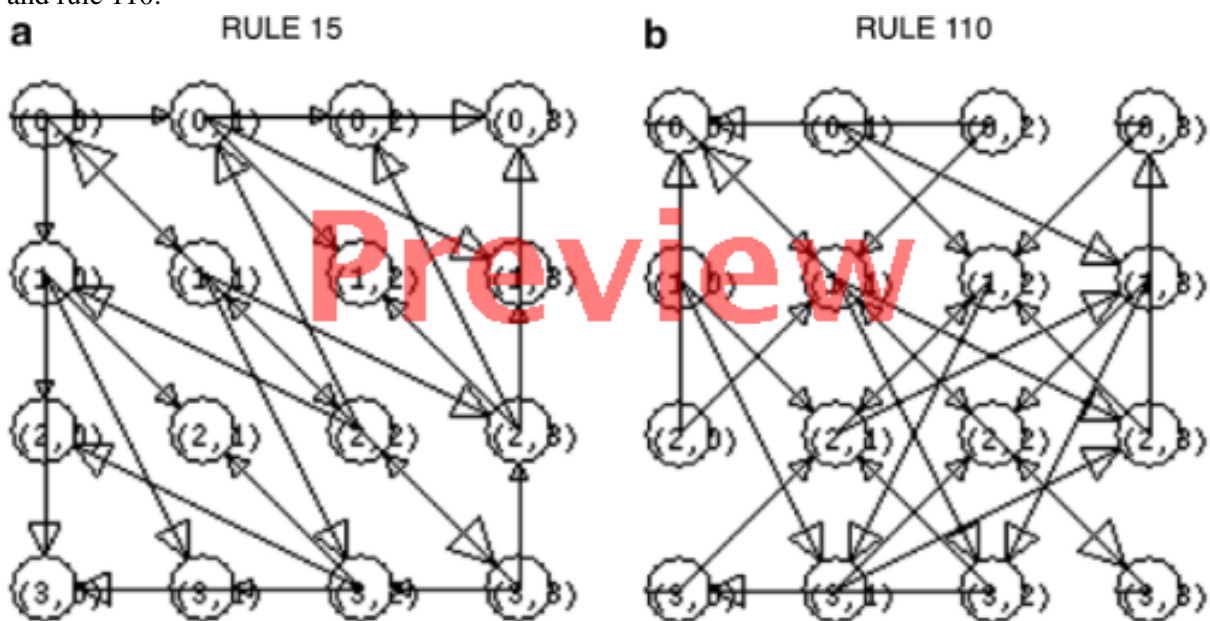
The evolution rule of a CA can be represented by a de Bruijn graph, in which vertices are the set of sequences in $V = S^{2r}$. For $w = w_1 \dots w_{2r}$ in S^{2r} , let us define $\alpha(w) = w_1 \dots w_{2r-1}$ and $\beta(w) = w_2 \dots w_{2r}$. For v and w in V , there is a directed edge from v to w if $\beta(v) = \alpha(w)$. In this way, every edge in the de Bruijn graph represents a complete neighborhood defined by the overlapping of $2r - 1$ cells from v to w . This edge is labeled by the evolution of the corresponding neighborhood given by $\varphi(v_1 \dots v_{2r} w_{2r})$. Figure 3 depicts the de Bruijn graphs for ECA rule 15 and rule 110.



If you need to edit the image, please use the original: 126766_0_En_677-1_Fig3_Print.tif

Fig. 3
De Bruijn graphs for ECA rule 15 (a) and rule 110 (b)

Given a de Bruin diagram, a new graph can be defined taking as vertices all the pairs of de Bruijn vertices. For de Bruijn nodes v, w, x, y , there is a directed edge in the pair graph from (v, w) to (x, y) if and only if $\varphi(v_1 x_1 \dots x_{2r}) = \varphi(w_1 y_1 \dots y_{2r})$. Figure 4 presents the pair graphs for ECA rule 15 and rule 110.

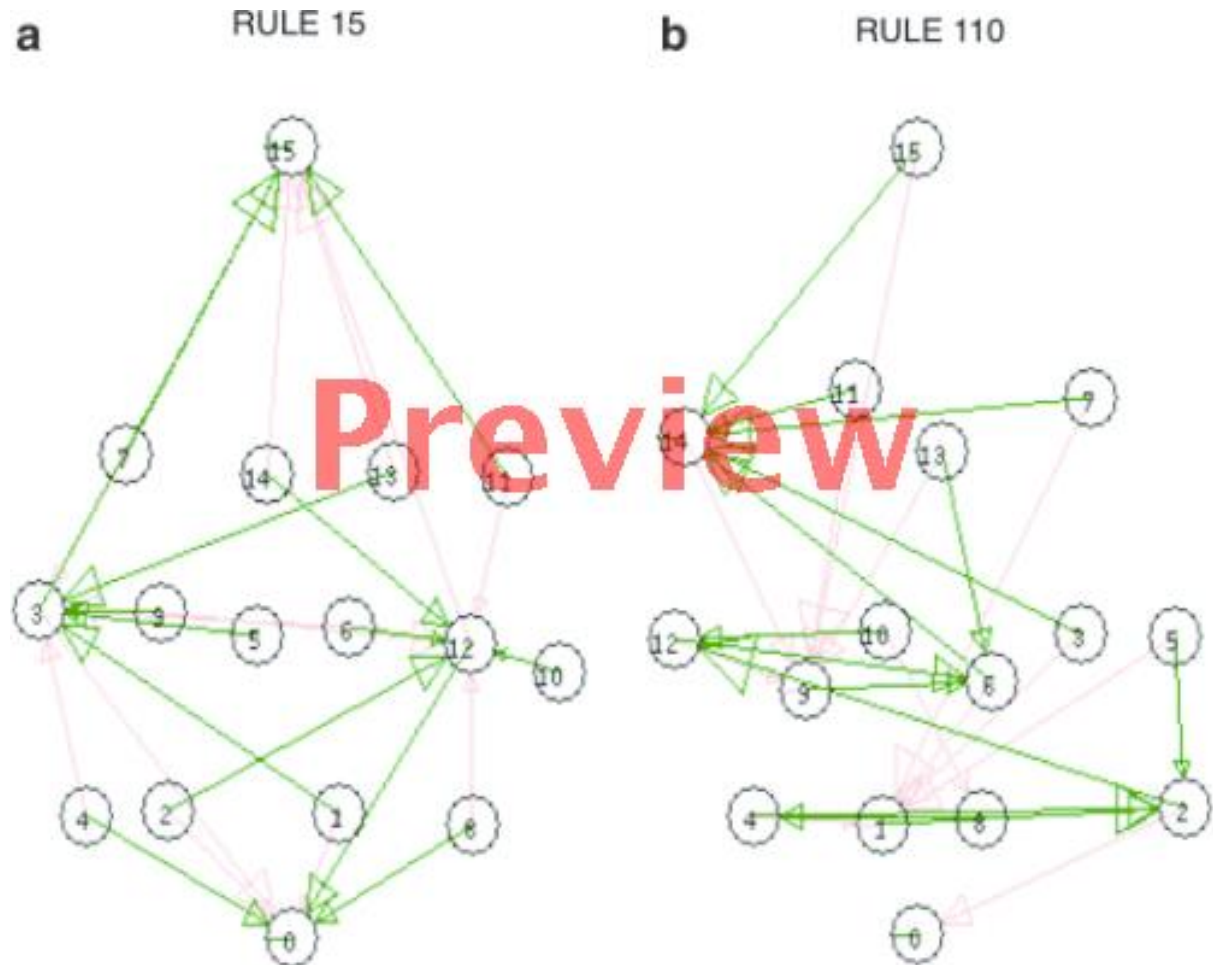


If you need to edit the image, please use the original: 126766_0_En_677-1_Fig4_Print.tif

Fig. 4
Pair graphs for ECA rule 15 (a) and rule 110 (b)

Another graphical construction derived from the de Bruijn graph is the power set of the vertices starting with the empty set. We shall define this set as \mathcal{P} such that every $P \in \mathcal{P}$ holds that $P \subseteq S$ and $|\mathcal{P}| = 2^{|S|}$. This subset construction (or subset graph) is defined taking \mathcal{P} as the set of vertices. For P, Q in \mathcal{P} , there is a directed edge from P to Q if for a given state $s \in S$ and for every $p \in P$ there is a $q \in Q$ such

that $\varphi(p_1 q_1 \dots q_{2r}) = s$, and Q is maximal. If for a given s we cannot find such a subset Q , then the directed edge goes from P to the empty set. Figure 5 presents the subset graphs for ECA rule 15 and rule 110.

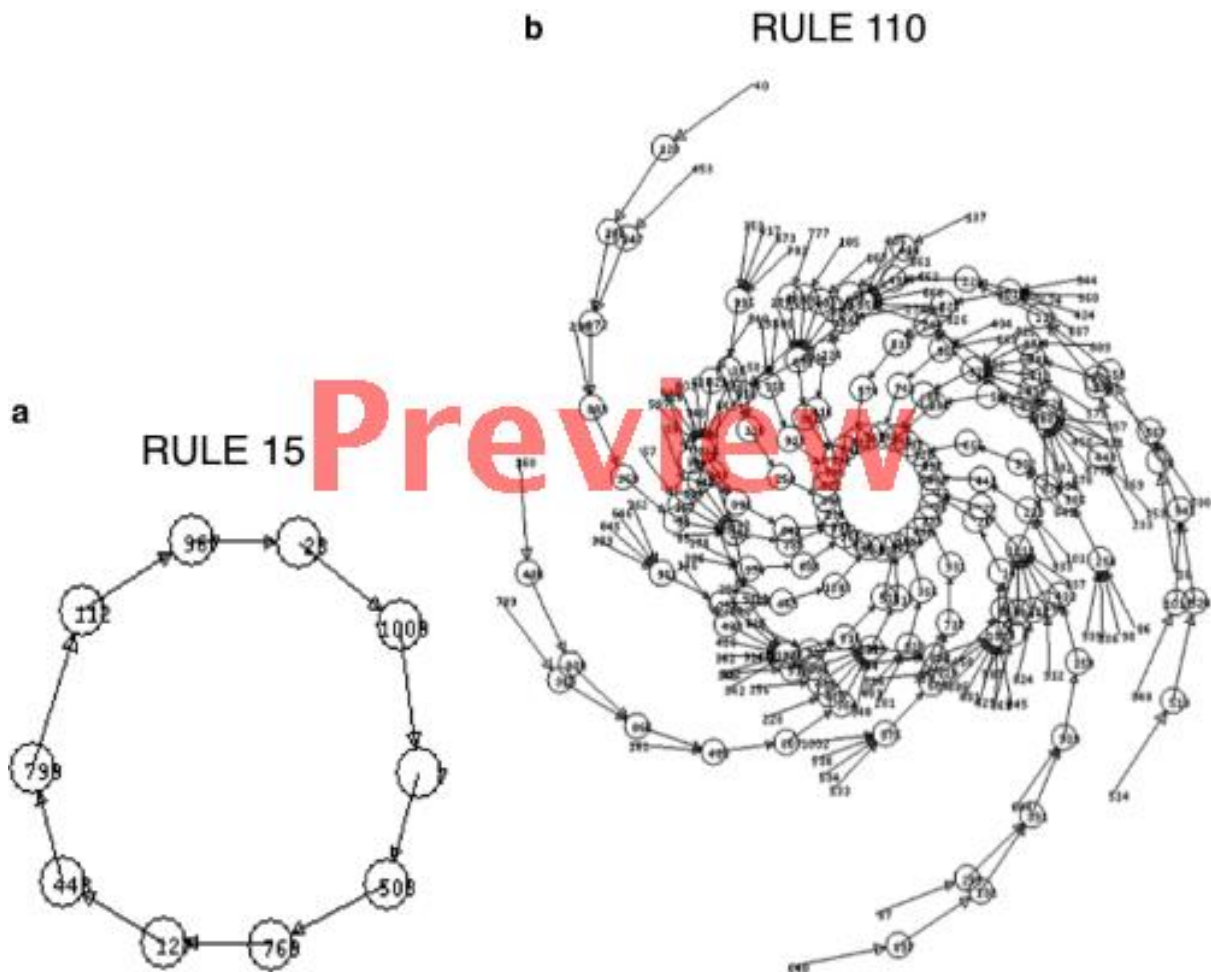


If you need to edit the image, please use the original: 126766_0_En_677-1_Fig5_Print.tif

Fig. 5
Subset graphs for ECA rule 15 (a) and rule 110 (b)

For configuration of n cells, periodic boundary conditions allow the specification of another graph, where vertices are the sequences in S^n . For configurations v, w in S^n , there is a directed edge from v into w if $\Phi(v) = w$.

This graph describes completely the global dynamics of a CA depicting the periodic behaviors starting from any initial configuration. These periodic behaviors are represented by cycles in the graph or basins of attraction, reason why this construction is called a cycle graph. Figure 6 shows part of the cycle graphs for ECA rule 15 and rule 110 taking configurations of 10 cells.



If you need to edit the image, please use the original: 126766_0_En_677-1_Fig6_Print.tif

Fig. 6
Cycle graphs for ECA rule 15 (a) and rule 110 (b)

De Bruijn Graph

Features of de Bruijn Graphs in Reversible Automata

Any reversible CA can be represented by another with both invertible rules with neighborhood size 2 Moore and Boykett ([1997](#)), Seck-Tuoh-Mora et al. ([2005](#)), Boykett et al. ([2008](#)). In this case, the corresponding de Bruijn graph holds three main properties established in Hedlund ([1969](#)):

1.

There are $|S|$ paths representing each sequence of states.

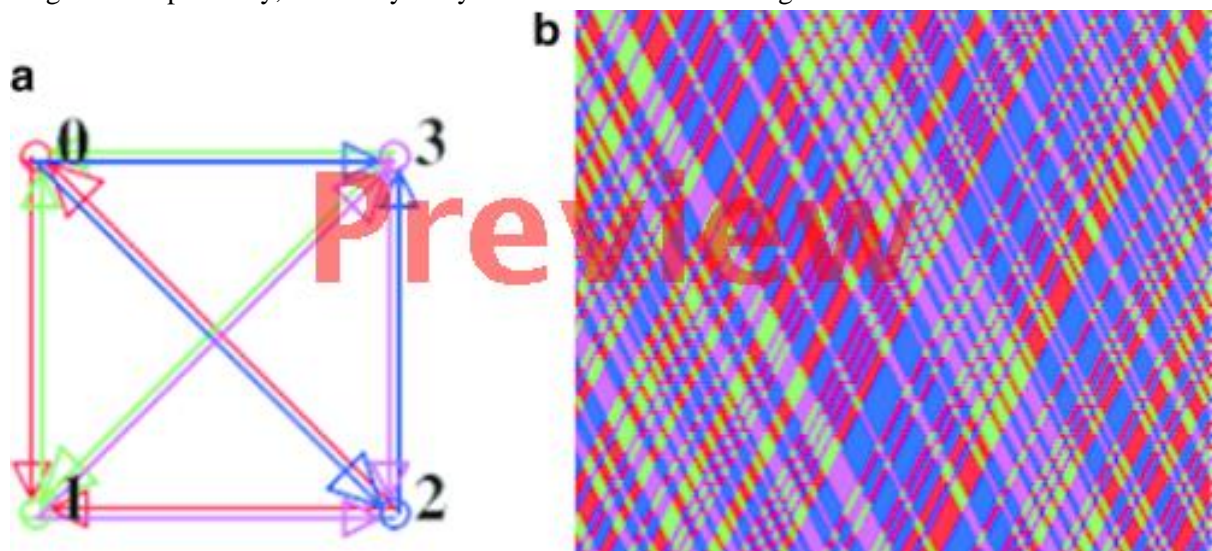
2.

These paths start from a set L of initial nodes and end into a set R of final nodes such that $|L| |R| = |S|$.

3.

There is a unique node v in $L \cap R$.

Figure 7 illustrates a spatial-temporal pattern and the de Bruijn graph for a reversible CA of four states and neighborhood size 2 (or neighborhood radius 1/2) for both invertible rules. The evolution rule is represented by a matrix where rows and columns indices represented the left and right neighbors respectively, and every entry is the evolution of the neighborhood.

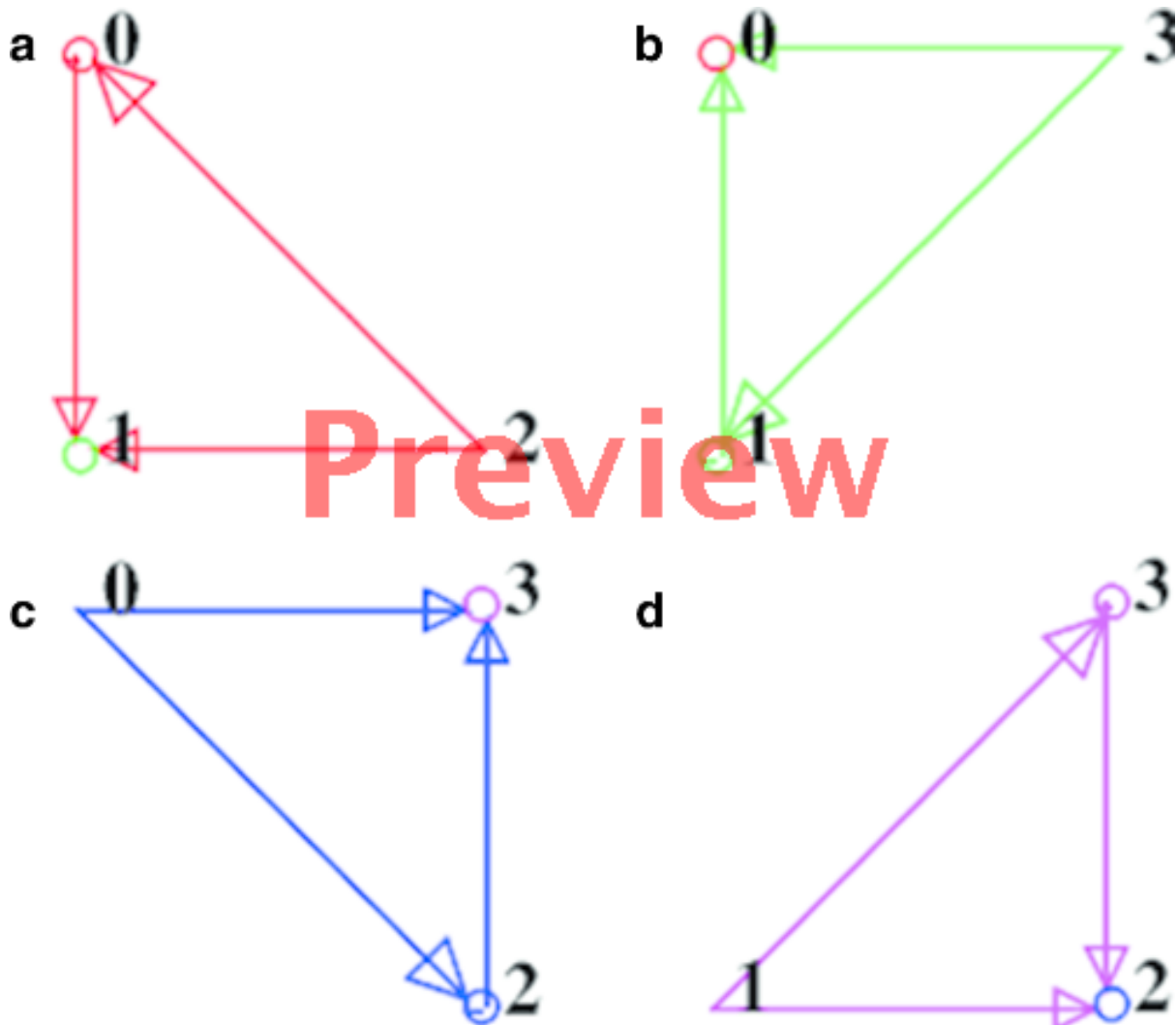


If you need to edit the image, please use the original: 126766_0_En_677-1_Fig7_Print.tif

Fig. 7

De Bruijn graph (**a**) and spatial-temporal pattern (**b**) for reversible CA 4 *h* rule F5A0F5A0

Figure 8 describes the paths for each state in the de Bruijn graph, which are consistent with the properties described above for reversible CA.



If you need to edit the image, please use the original: 126766_0_En_677-1_Fig8_Print.tif

Fig. 8

Paths for state 1 (a), 2 (b), 3 (c), and 4 (d) for the de Bruijn graph of reversible CA 4 *h* rule F5A0F5A0

Features of de Bruijn Graphs in Complex Automata

The de Bruijn graphs are very useful to determine all possible strings that represent nontrivial or complex patterns known as gliders, particles, waves, or mobile self-localizations in complex rules. After the de Bruijn graphs are completed, we can calculate an extended de Bruijn graph. An extended de Bruijn graph takes into account more significant overlapping of neighborhoods of length $2r$. We represent $M^{(2)}$ by indexes $i = j = 2r * n$, where $n \in \mathbb{Z}^+$. The de Bruijn graph grows exponentially, order $\left(\{k\}^{2\{r\}^n} \right)$, for each $M^{(n)}$. Specifically, extended de Bruijn graphs calculate strings that are periodic; these strings are regular expressions that can be coded by concatenations into an initial condition to collide gliders in different phases.

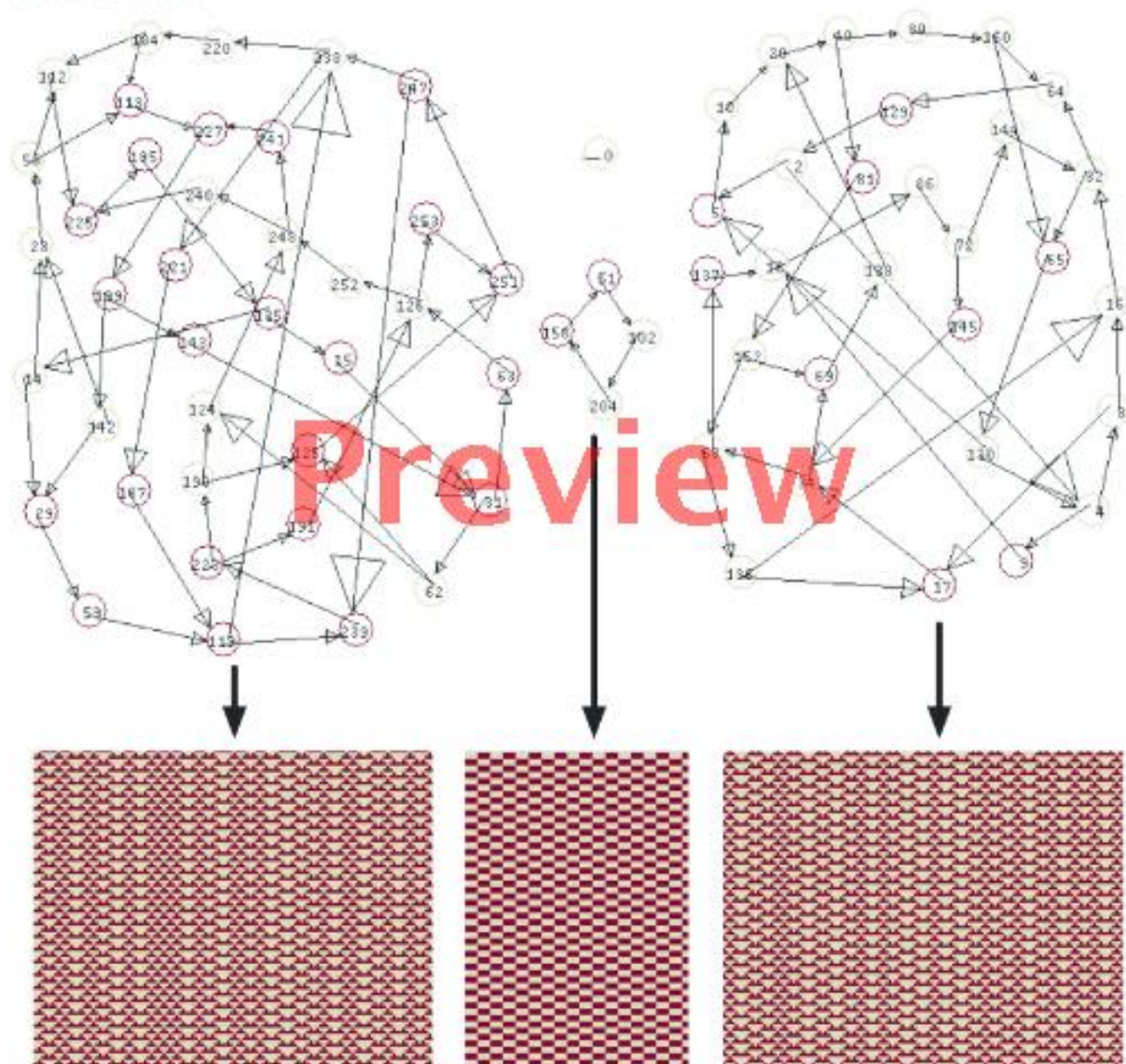
For ECA the module $k^2r = 2^2 = 4$ represents the number of vertexes in the de Bruijn graph and j takes values from $k * i = 2i$ to $(k * i) + k * 1 = (2 * i) + 2 - 1 = 2i + 1$. The vertexes (indexes of a matrix M) are labeled by fractions of neighborhoods beginning with 00, 01, 10, and 11; the overlap determines each connection completing every neighborhood. Paths in the de Bruijn graph represent

strings, configurations, or fragment of configurations in the evolution space. Also fragments of the diagram itself are useful in discovering periodic blocks of more small strings, ancestors, and cycles. In these graphs we can find systematically any periodic structure, including some gliders.

For extended de Bruijn graphs we have shift registers to the right (+) or to the left (-). A glider can be identified as a cycle and the glider interaction will be a connection with other cycles. Diagram (2, 2) (x -displacements, y -generations) displays periodic strings moving two cells to the right in two time steps, i.e., period of a glider. This way, we can enumerate each string for every structure in this domain.

The de Bruijn graph that can calculate stationary pattern is of order $\lfloor (M)_{R54}^{(4)} \rfloor$ because these gliders have period four without displacements. These patterns can be considered also as still life configurations. Figure 9 shows the full de Bruijn graph (0,4) used to calculate these stationary patterns. There are four main cycles: two largest cycles represent phases of each stationary pattern plus its periodic background, and two smaller cycles characterizing two different periodic patterns in rule 54 including the stable state represented with a loop by vertex zero. Space-time configurations of ECA derived from these diagrams are illustrated on the left plate of Fig. 9. Position of each glider and periodic background follows arbitrarily routes into these cycles. Details on these regular expressions for rule 54 are presented in Martínez et al. (2014).

shift 0 in 4 gen



If you need to edit the image, please use the original: 126766_0_En_677-1_Fig9_Print.tif

Fig. 9

Extended de Bruijn graphs calculating periodic patterns with zero displacement in four generations for ECA rule 54. Every cycle is showed below every diagram. This way, patterns are defined as a code since its initial condition obtained from diagram

De Bruijn diagrams contain all relevant information about complex patterns emerging in CAs. The de Bruijn diagrams can proof exhaustively the number of periodic patterns that a rule can yield. As a generality, reversible or class II CAs refer de Bruijn graphs with disjoint cycles, while complex rules contain cycles that can be interconnected jumping between them. Regularly these interconnections imply a change of phase from a glider to other glider or a stable periodic background.

Relevant References in Reversibility and Complexity Using de Bruijn Diagrams

The chaotic discrete characteristics of ECA Rule 126 are analyzed using de Bruijn diagrams in Martínez et al. ([2010](#)). It is shown in Nobe and Yura ([2004](#)) that there exist exactly 16 reversible ECA rules for infinitely many cell sizes by means of a correspondence between ECAs and de Bruijn graphs. Glider coding in initial conditions by means of a finite subset of regular expressions extracted from de Bruijn graphs is explained in Martínez et al. ([2008](#)). De Bruijn graphs and their fragment matrices are applied for testing linearity and computation of the Z parameter, and the construction of adjacency matrices for transition diagrams is presented in Voorhees ([2008](#)). De Bruijn graphs are used in Martinez et al. ([2013](#)) to examine CAs belonging to Class III (in Wolfram's classification) that are capable of universal computation. De Bruijn graphs are discussed in Betel et al. ([2013](#)) to treat the parity problem in one-dimensional, binary CAs for different radius sizes. A method proposed to calculate preimages in one-dimensional CAs using de Bruijn graphs for any k -states and r -radius using the classic path-finding problem in graph theory is described in Soto ([2008](#)), and other methods of finding the total number of preimages for a given homogeneous configuration is described in Powley and Stepney ([2010](#)). Reachability tree developed from de Bruijn graphs which represents all possible reachable configurations of a CA is explained in Bhattacharjee and Das ([2016](#)) to test reversibility. De Bruijn graphs are used in reversible one-dimensional CAs to prove that they are equivalent to the full shift in Seck-Tuoh-Mora et al. ([2003a](#)) and Seck-Tuoh-Mora et al. ([2003b](#)). De Bruijn graphs for analysis of two evolution rules in two dimensions (Conway's Game of Life and the quasi-chaotic Diffusion Rule) are explained in McIntosh ([2010](#)) and Leon and Martinez ([2016](#)). An analysis of traffic models based on one-dimensional CAs with de Bruijn graphs is developed in Zamora and Vergara ([2004](#)).

Pair and Subset Graphs

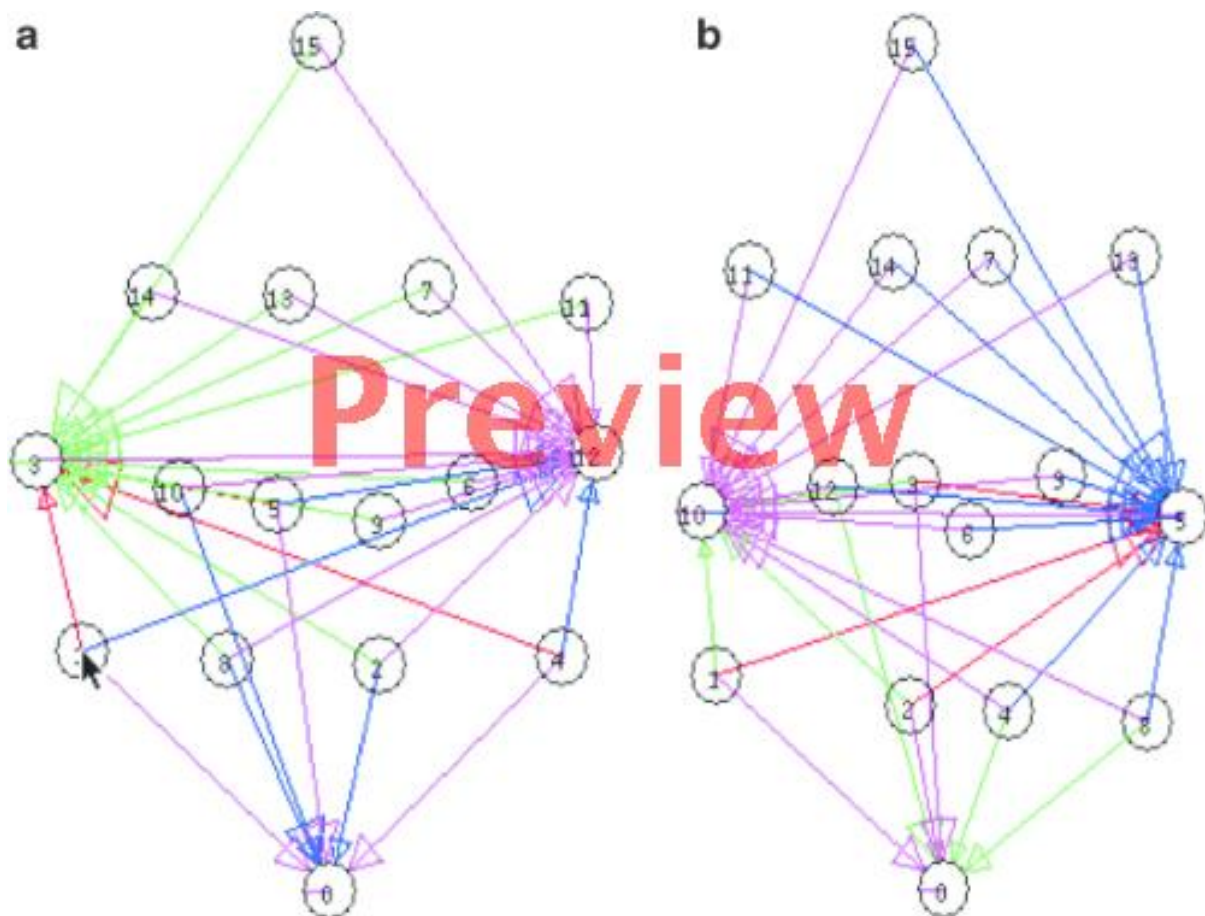
Features of Subset Graphs in Surjective Automata

Reversible CA is a special kind of surjective automaton where every sequence has a possible preimage, that is, there is no Garden-of-Eden configurations McIntosh ([2009](#)). Surjective automata

can be detected using the subset graph, a CA is surjective if there are no paths starting from the complete subset and finishing in the empty set.

In reversible CA, the paths in the subset graph starting from the complete subset will end into subsets $W \subseteq S$ such that $|W| = |R|$. That is because the ending nodes of the paths represent the right neighbors of a given sequence, and the properties of reversible automata indicate that the number of possible rightmost cells in the preimages of every sequence is $|R|$. If we take the opposite direction of the edges in the de Bruijn graph and construct the corresponding subset graph, a similar effect is obtained but now the ending nodes $W' \subseteq S$ denote the leftmost cells in the preimages of every sequence, and $|W'| = |L|$.

Figure 10 presents the subset graphs taking the forward and backward direction of the edges in the de Bruijn graph. Nodes are enumerated in base 4 according to the elements belonging to each subset. Note that in both cases, the ending nodes have a cardinality $|L| = |R| = 2$, fulfilling that $|L| + |R| = |S| = 4$.



If you need to edit the image, please use the original: 126766_0_En_677-1_Fig10_Print.tif

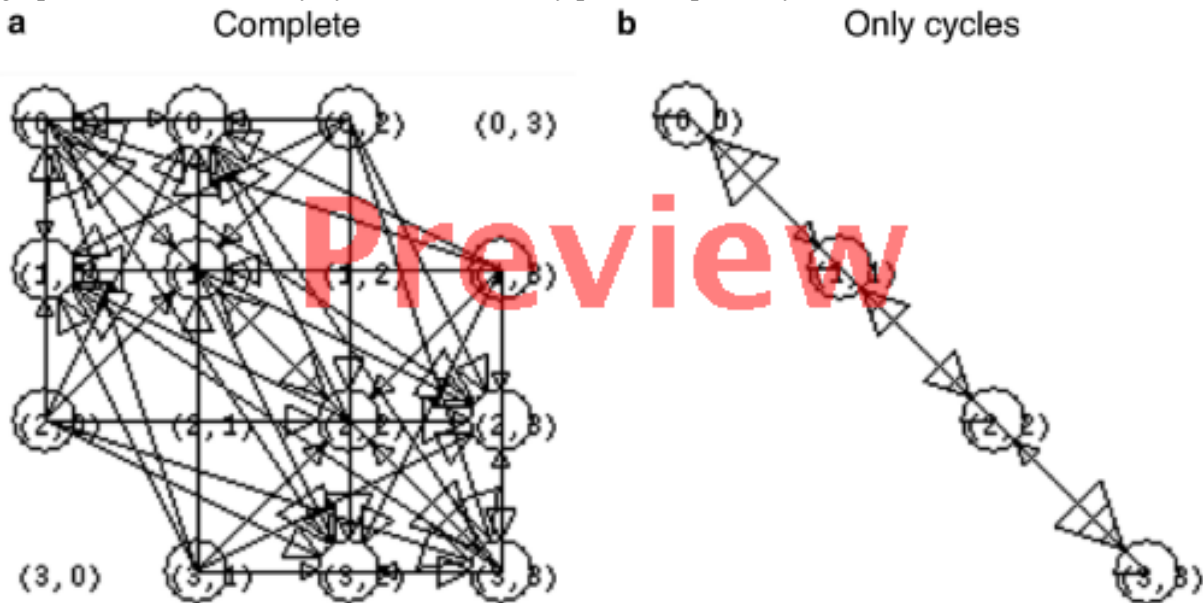
Fig. 10

Subset graphs for reversible CA 4 h rule F5A0F5A0 taking the forward (**a**) and backward (**b**) direction of the edges in the de Bruijn graph

Features of Pair Graphs in Reversible Automata

The pair graph offers a direct way to check reversibility in one-dimensional CAs with quadratic complexity. If there are only cycles defined by the nodes composed by pairs of identical elements, it

means that there is no sequence with different preimages taking periodic boundary conditions. Figure 11 presents the pair graph (complete and only cycles) generated taking pairs of nodes in the de Bruijn graph. Notice that the only cycles are defined by pairs composed by identical elements.



If you need to edit the image, please use the original: 126766_0_En_677-1_Fig11_Print.tif

Fig. 11

Pair graphs (complete (a) and only cycles (b)) for reversible CA 4 h rule F5A0F5A0

Features of Subset Graphs in Complex Automata

The subset graph also is useful as a deterministic finite state machine for the language of a specific CA. If a string belongs to a language determined for a CA given, there is a way in the subset graph avoiding the empty set. In this case, every vertex can represent an accepting state excluding the empty set, and the initial state the maximum subset.

When in reversible CA some vertexes work as attractors (called index Welch's Seck-Tuoh-Mora et al. (2003b)), in complex rules you should find ways from the maximum subset to the empty set. These ways represent strings without ancestors for this CA, these strings are known as Garden-of-Eden configurations. Frequently, from von Neumann CA and several computable conventional CA, they have Garden-of-Eden configurations including the Game of Life and ECA rule 110.

For example, the expression 11111000111000100110 represents a glider with positive slope moving in ECA rule 110. Concatenations of these strings will yield a periodic evolution space covered just with this glider. Following a way in its subset graph, we can prove that this regular expression is recognized for the language of periodic structures derived for the rule 110. Particularly, this string has the next route in the subset diagram Fig. 5, as follows: $15 \rightarrow 14 \rightarrow 14 \rightarrow 14 \rightarrow 14 \rightarrow 14 \rightarrow 9 \rightarrow 9 \rightarrow 9 \rightarrow 6 \rightarrow 14 \rightarrow 14 \rightarrow 9 \rightarrow 9 \rightarrow 9 \rightarrow 6 \rightarrow 1 \rightarrow 1 \rightarrow 2 \rightarrow 12 \rightarrow 9$.

Relevant References in Reversibility and Complexity Using Pair and Subset Graphs

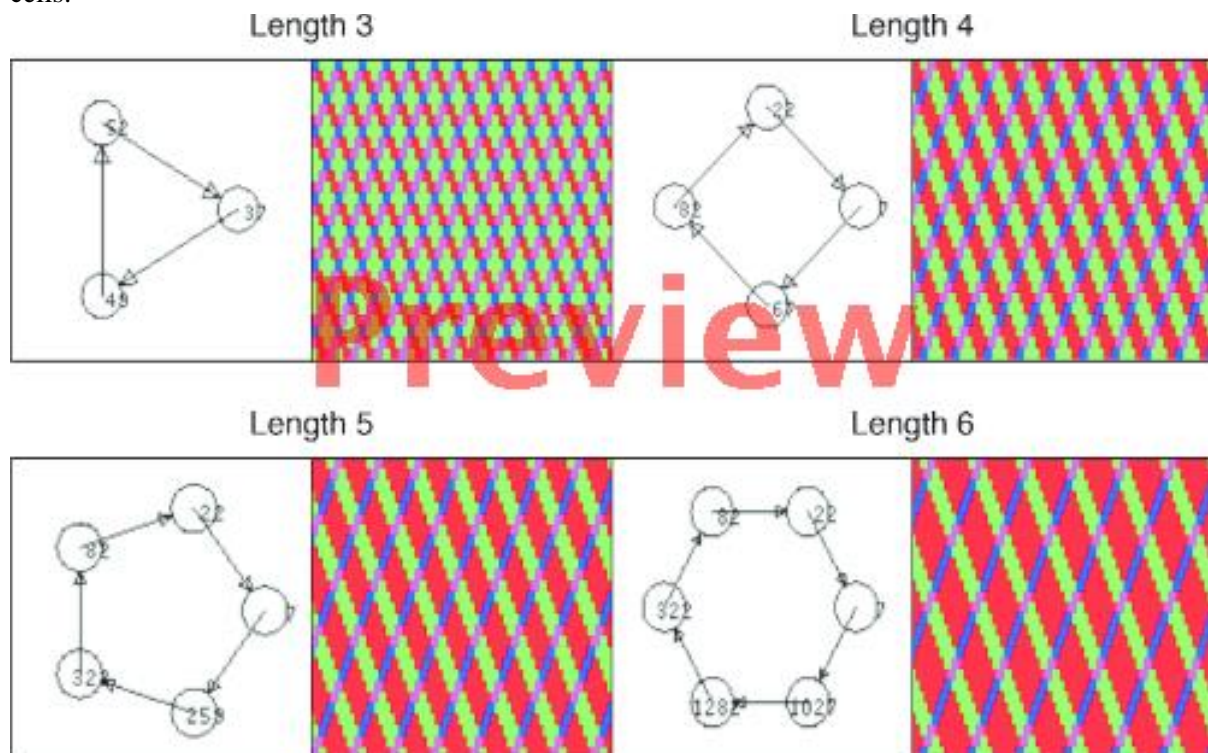
A procedure to calculate preimages for a given sequence of states based on the subset graph is presented in Seck-Tuoh-Mora et al. (2004). An analysis of procedures to calculate preimages based on de Bruijn and subset graphs is developed in Jeras and Dobnikar (2007). Concepts of the subset graph are used to tackle the reversibility problem of all 1D linear CA rules over $Z(2)$ under null boundary conditions in Yang et al. (2015). The pair graph is used in Seck-Tuoh-Mora et al. (2008) for knowing the size of the inverse neighborhood and obtaining the inverse local rule in reversible automata. A graph-theoretical approach related to de Bruijn and pair graphs to characterize reversible CAs is described in Moraal (2000).

Cycles and Basins of Attraction

Features of Cycle Graphs in Reversible Automata

The cycle graph that is associated with a reversible automaton is characterized to be composed by only cycles and no branches, due to every finite configuration has only one and only one preimage taking periodic boundary conditions.

The length of every cycle gives the periodicity of the configurations composing it. Figure 12 describes some cycle graphs for different configuration lengths. These configurations can be periodically repeated in a larger configuration to obtain regular spatial-temporal patterns with larger number of cells.



If you need to edit the image, please use the original: 126766_0_En_677-1_Fig12_Print.tif

Fig. 12

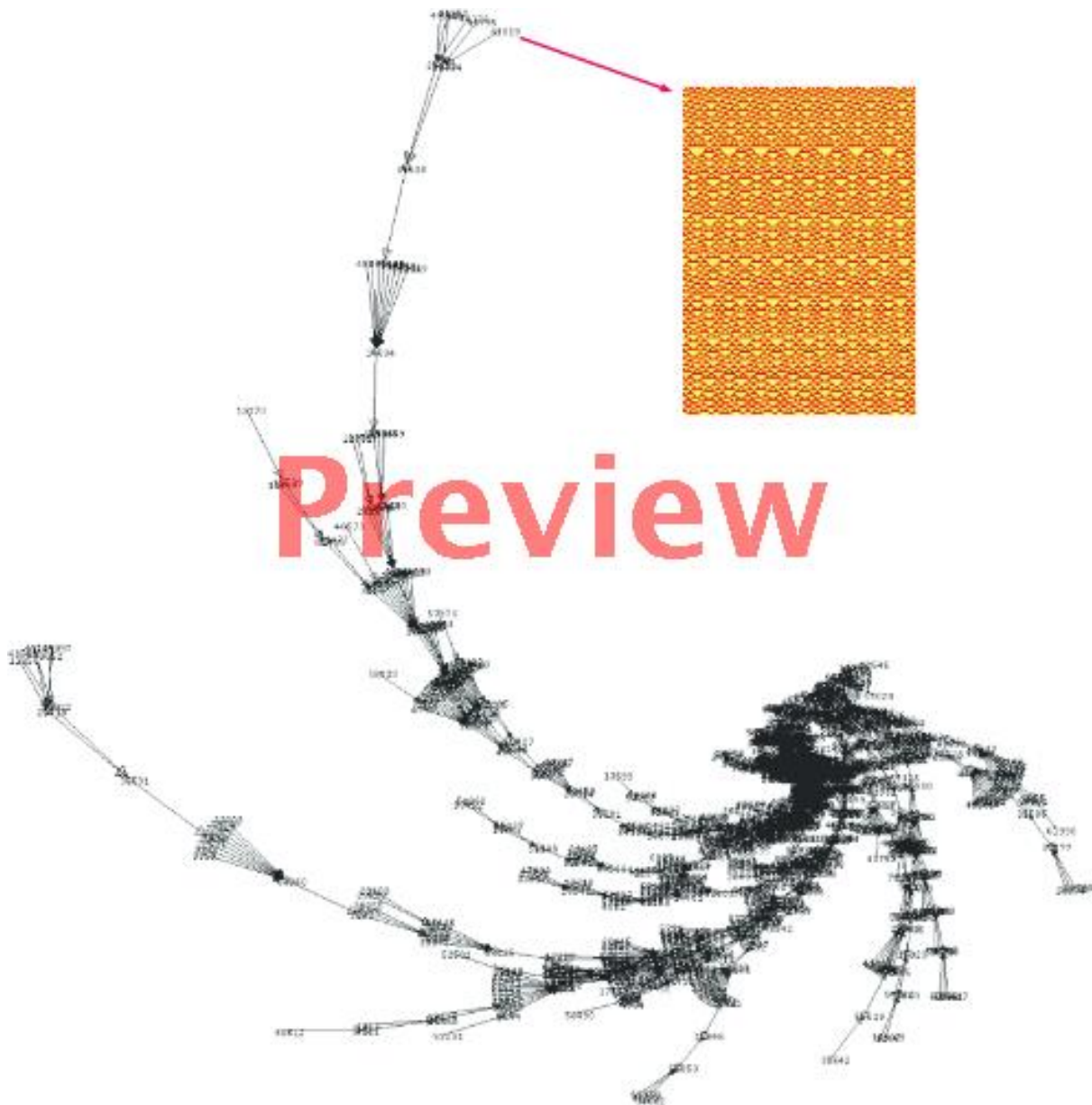
Cycle graphs with different configuration lengths for reversible CA 4 h rule F5A0F5A0

Features of Cycle Diagrams in Complex Automata

Another way to get periodic structures in CA is calculating the cycle diagrams (or attractors). Indeed, Wuensche in Wuensche and Lesser ([1992](#)) did a detailed analysis offering an ECA classification based in basins of attraction properties.

Wuensche establishes that possible complex CA must have moderate number of transients, moderate length in its period, moderate depth, and moderate density. However, we can see which cycle diagrams follow other structures that typically uniform, periodic, or chaotic CA not. Attractors in complex CA display nonsymmetric histories (branches), and a second feature is that these three have long transients.

As an example, Fig. [13](#) displays a basin of attraction for configurations with 16 cells. This cycle diagram contains a mass of 1,246 configurations and a period in its attractor of 40 configurations. Maximum high in this tree has 32 transients before to reach the attractor. Particularly, if we concatenate the leaf 41,819 on the initial condition its evolution will converge to a meta-glider in ECA rule 54 preserved by multiple collisions between three gliders Martínez et al. ([2014](#)). Extended analysis with cycle diagrams implies meta diagrams interconnecting not configuration but basins of attractions, where complex rules display diagrams strongly connected Martínez et al. ([2017](#)).



If you need to edit the image, please use the original: [126766_0_En_677-1_Fig13_Print.tif](#)

Fig. 13

Cycle graph calculating gliders in the complex ECA rule 54. The cycle graph has a mass of 1,246 vertexes and a period of 40 configurations. In the top right side a fragment of evolution displays its dynamics starting from a leaf, the configuration number 41,819

Relevant References in Reversibility and Complexity Using Cycle Graphs

DDLab is an interactive graphics software for creating and visualizing discrete dynamical networks, and studying their behavior in terms of both space-time patterns and basins of attraction Wuensche ([2005](#)). It is shown in Pei et al. ([2014](#)) that there exist two Bernoulli-measure attractors in ECA rule 58. The dynamical properties of topological entropy and topological mixing of rule 58 are described using cycle graphs for small configurations. Cycle periods of the Baker transformation and

equivalence classes in CAs are discussed in Voorhees ([2006](#)). The contribution of cycles of any length for sustaining network activity and a refined mean-field approach is developed in Garcia et al. ([2014](#)). The limit set of 104 asynchronous ECAs over the cycle graphs on n vertices is considered in Macauley and Mortveit ([2013](#)). Cycle graph equivalence of asynchronous CAs is studied in Macauley and Mortveit ([2009](#)). The dynamics of cycle graphs is reinterpreted by interpolation surfaces in Seck-Tuoh-Mora et al. ([2014](#)). The basin tree diagrams and the portraits of the omega-limit orbits of CAs with permutative rules are classified in Chua and Paziienza ([2009](#)) and revised in Chua et al. ([2006](#)) for reversible automata. A classification of CAs according to the complexities which rise from the basins of attraction of subshift attractors is investigated in Di Lena and Margara ([2008](#)). An analysis of nonuniform CAs with associative memory using basins of attraction is developed in Maji and Chaudhuri ([2008](#)). Basins of attraction and the density classification problem for CAs are investigated in Bossomaier et al. ([2000](#)). Cycle graphs of linear CAs and the characterization of their connected components as direct sums are treated in Chin et al. ([2001](#)).

Future Directions

This contribution has presented the basics of de Bruijn, pair, subset and cycle graphs, and a brief review of relevant works applying them in the study of one-dimensional CAs.

The matrix analysis is an important tool to characterize and understand deeper properties of graphs. Further directions in the study of de Bruijn graphs may be the application of spectral analysis to explore the results in this area in the investigation of CAs.

Symbolic dynamics is another important tool in the dynamical analysis of CAs. Links between symbolic dynamics and the graphs presented in this work could enrich the application of graphical tools for the analysis of CAs.

The extension of graphs in more dimensions is another opportunity of future research in this field. Some results using de Bruijn graphs have been presented in this work; however, there is an unopened field of research using graphs for reversible and complex automata in two and more dimensions. Of course, there is an exponential growth in the size of the involved graphs, nevertheless, the computational resources nowadays make possible this kind of study.

Bibliography

Primary Literature

Bang-Jensen J, Gutin GZ (2008) Digraphs: theory, algorithms and applications. Springer, London

Betel H, de Oliveira PP, Flocchini P (2013) Solving the parity problem in one-dimensional cellular automata. *Nat Comput* 12(3):323–337

[MathSciNet](#) [MATH](#) [CrossRef](#)

Bhattacharjee K, Das S (2016) Reversibility of d -state finite cellular automata. *J Cell Autom* 11:213–245

[MathSciNet](#)

Bossomaier T, Sibley-Punnett L, Cranny T (2000) Basins of attraction and the density classification problem for cellular automata. In: International conference on virtual worlds, Springer, pp 245–255

Boykett T, Kari J, Taati S (2008) Conservation laws in rectangular ca. *J Cell Autom* 3(2):115–122

de Bruijn N (1946) A combinatorial problem. *Proc Sect Sci Kon Akad Wetensch Amsterdam* 49(7):758–764

[MATH](#)

Chin W, Cortzen B, Goldman J (2001) Linear cellular automata with boundary conditions. *Linear Algebra Appl* 322(1–3):193–206

[MathSciNet](#) [MATH](#) [CrossRef](#)

Chua LO, Paziienza GE (2009) A nonlinear dynamics perspective of wolfram’s new kind of science part xii: period-3, period-6, and permutive rules. *Int J Bifurcation Chaos* 19(12):3887–4038

[MATH](#) [CrossRef](#)

Chua LO, Sbitnev VI, Yoon S (2006) A nonlinear dynamics perspective of wolfram’s new kind of science part vi: from time-reversible attractors to the arrow of time. *Int J Bifurcation Chaos* 16(05):1097–1373

[MATH](#) [CrossRef](#)

Di Lena P, Margara L (2008) Computational complexity of dynamical systems: the case of cellular automata. *Inf Comput* 206(9–10):1104–1116

[MathSciNet](#) [MATH](#) [CrossRef](#)

Garcia GC, Lesne A, Hilgetag CC, Hütt MT (2014) Role of long cycles in excitable dynamics on graphs. *Phys Rev E* 90(5):052,805

[CrossRef](#)

Golomb SW et al (1982) Shift register sequences. World Scientific, Singapore

Hedlund GA (1969) Endomorphisms and automorphisms of the shift dynamical system. *Theor Comput Syst* 3(4):320–375

[MathSciNet MATH](#)

Hopcroft JE (1979) Introduction to automata theory, languages and computation. Addison-Wesley, Boston

Jen E (1987) Scaling of preimages in cellular automata. *Complex Syst* 1:1045–1062

[MathSciNet MATH](#)

Jeras I, Dobnikar A (2007) Algorithms for computing preimages of cellular automata configurations. *Phys D* 233(2):95–111

[MathSciNet MATH CrossRef](#)

Khoussainov B, Nerode A (2001) Automata theory and its applications, vol 21. Springer, New York

Leon PA, Martinez GJ (2016) Describing complex dynamics in lifelike rules with de Bruijn diagrams on complex and chaotic cellular automata. *J Cell Autom* 11(1):91–112

Macauley M, Mortveit HS (2009) Cycle equivalence of graph dynamical systems. *Nonlinearity* 22(2):421

[ADS MathSciNet MATH CrossRef](#)

Macauley M, Mortveit HS (2013) An atlas of limit set dynamics for asynchronous elementary cellular automata. *Theor Comput Sci* 504:26–37

[MathSciNet MATH CrossRef](#)

Maji P, Chaudhuri PP (2008) Non-uniform cellular automata based associative memory: evolutionary design and basins of attraction. *Inf Sci* 178(10):2315–2336

[MathSciNet MATH CrossRef](#)

Martínez GJ, McIntosh HV, Seck Tuoh Mora JC, Chapa Vergara SV (2008) Determining a regular language by glider-based structures called phases $f(i)_1$ in rule 110. *J Cell Autom* 3(3):231

[MathSciNet MATH](#)

Martínez GJ, Adamatzky A, Seck-Tuoh-Mora JC, Alonso-Sanz R (2010) How to make dull cellular automata complex by adding memory: rule 126 case study. *Complexity* 15(6):34–49

[MathSciNet](#)

Martínez GJ, Mora JC, Zenil H (2013) Computation and universality: class iv versus class iii cellular automata. *J Cell Autom* 7(5–6):393–430

[MathSciNet](#) [MATH](#)

Martínez GJ, Adamatzky A, McIntosh HV (2014) Complete characterization of structure of rule 54. *Complex Syst* 23(3):259–293

[MathSciNet](#) [MATH](#)

Martínez GJ, Adamatzky A, Chen B, Chen F, Seck JC (2017) Simple networks on complex cellular automata: from de Bruijn diagrams to jump-graphs. In: *Swarm dynamics as a complex networks*. Springer (To be published), pp 177–204

McIntosh HV (1991) Linear cellular automata via de Bruijn diagrams. Webpage:

<http://delta.cs.cinvestav.mx/~mcintosh>

McIntosh HV (2009) *One dimensional cellular automata*. Luniver Press, United Kingdom

McIntosh HV (2010) Life's still lifes. In: *Game of life cellular automata*. Springer, London, pp 35–50

Moore EF (1956) Gedanken-experiments on sequential machines. *Autom Stud* 34:129–153

[MathSciNet](#)

Moore C, Boykett T (1997) Commuting cellular automata. *Complex Syst* 11:55–64

[MathSciNet](#) [MATH](#)

Moraal H (2000) Graph-theoretical characterization of invertible cellular automata. *Phys D* 141(1):1–18

[ADS](#) [MathSciNet](#) [MATH](#) [CrossRef](#)

Mortveit H, Reidys C (2007) *An introduction to sequential dynamical systems*. Springer, New York

Nasu M (1977) Local maps inducing surjective global maps of one-dimensional tessellation automata. *Math Syst Theor* 11(1):327–351

[MathSciNet](#) [MATH](#) [CrossRef](#)

Nobe A, Yura F (2004) On reversibility of cellular automata with periodic boundary conditions. *J Phys A Math Gen* 37(22):5789
[ADS MathSciNet](#) [MATH CrossRef](#)

Pei Y, Han Q, Liu C, Tang D, Huang J (2014) Chaotic behaviors of symbolic dynamics about rule 58 in cellular automata. *Math Probl Eng* 2014:Article ID 834268, 9 pages

Powley EJ, Stepney S (2010) Counting preimages of homogeneous configurations in 1-dimensional cellular automata. *J Cell Autom* 5(4–5):353–381
[MathSciNet](#) [MATH](#)

Rabin MO, Scott D (1959) Finite automata and their decision problems. *IBM J Res Develop* 3(2):114–125
[MathSciNet](#) [MATH CrossRef](#)

Sakarovitch J (2009) *Elements of automata theory*. Cambridge University Press, New York

Seck-Tuoh-Mora JC, Hernández MG, Martínez GJ, Chapa-Vergara SV (2003a) Extensions in reversible one-dimensional cellular automata are equivalent with the full shift. *Int J Mod Phys C* 14(08):1143–1160
[CrossRef](#)

Seck-Tuoh-Mora JC, Hernández MG, Vergara SVC (2003b) Reversible one-dimensional cellular automata with one of the two welch indices equal to 1 and full shifts. *J Phys A Math Gen* 36(29):7989
[ADS MathSciNet](#) [MATH CrossRef](#)

Seck-Tuoh-Mora JC, Martínez GJ, McIntosh HV (2004) Calculating ancestors in one-dimensional cellular automata. *Int J Mod Phys C* 15(08):1151–1169
[MATH CrossRef](#)

Seck-Tuoh-Mora JC, Vergara SVC, Martínez GJ, McIntosh HV (2005) Procedures for calculating reversible one-dimensional cellular automata. *Phys D* 202(1):134–141
[MathSciNet](#) [MATH CrossRef](#)

Seck-Tuoh-Mora JC, Hernández MG, Chapa Vergara SV (2008) Pair diagram and cyclic properties characterizing the inverse of reversible automata. *J Cell Autom* 3(3):205–218

Seck-Tuoh-Mora JC, Medina-Marin J, Martínez GJ, Hernández-Romero N (2014) Emergence of density dynamics by surface interpolation in elementary cellular automata. *Commun Nonlinear Sci Numer Simul* 19(4):941–966
[ADS MathSciNet CrossRef](#)

Shannon CE (2001) A mathematical theory of communication. *ACM SIGMOBILE Mobile Comput Commun Rev* 5(1):3–55
[MathSciNet CrossRef](#)

Soto JMG (2008) Computation of explicit preimages in one-dimensional cellular automata applying the de Bruijn diagram. *J Cell Autom* 3(3):219–230
[MathSciNet MATH](#)

Sutner K (1991) De Bruijn graphs and linear cellular automata. *Complex Syst* 5(1):19–30
[MathSciNet MATH](#)

Voorhees B (2006) Discrete baker transformation for binary valued cylindrical cellular automata. In: *International conference on cellular automata*, Springer, pp 182–191

Voorhees B (2008) Remarks on applications of de Bruijn diagrams and their fragments. *J Cell Autom* 3(3):187
[MathSciNet MATH](#)

Wolfram S (1984) Computation theory of cellular automata. *Commun Math Phys* 96(1):15–57
[ADS MathSciNet MATH CrossRef](#)

Wuensche A (2005) Discrete dynamics lab: tools for investigating cellular automata and discrete dynamical networks, updated for multi-value, section 23, chain rules and encryption. In: Adamatzky A, Komosinski M (eds) *Artificial life models in software*, Springer-Verlag, London, pp 263–297

Wuensche A, Lesser M (1992) The global dynamics of cellular automata: an atlas of basin of attraction fields of one-dimensional cellular automata. Addison-Wesley, Boston

Yang B, Wang C, Xiang A (2015) Reversibility of general 1d linear cellular automata over the binary field \mathbb{Z}_2 under null boundary conditions. *Inf Sci* 324:23–31
[ADS CrossRef](#)

Zamora RR, Vergara SVC (2004) Using de Bruijn diagrams to analyze 1d cellular automata traffic models. In: *International conference on cellular automata*, Springer, pp 306–315

Books and Reviews

Adamatzky A (ed) (2010) *Game of life cellular automata*, vol 1. Springer, London

Gutowitz H (1991) *Cellular automata: theory and experiment*. MIT Press, Cambridge, Massachusetts

Kari J (2005) Theory of cellular automata: a survey. *Theor Comput Sci* 334(1–3):3–33
[MathSciNet](#) [MATH](#) [CrossRef](#)

Toffoli T, Margolus NH (1990) Invertible cellular automata: a review. *Phys D* 45(1–3):229–253
[MathSciNet](#) [MATH](#) [CrossRef](#)